

## Targeting the Hinge Glycine Flip and the Activation Loop: Novel Approach to Potent p38 $\alpha$ Inhibitors

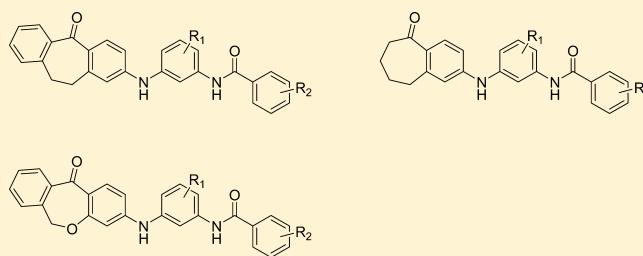
Kathrin E. Martz,<sup>†</sup> Angelika Dorn,<sup>†</sup> Benjamin Baur,<sup>†</sup> Verena Schattel,<sup>†</sup> Márcia I. Goettert,<sup>†</sup> Svenja C. Mayer-Wrangowski,<sup>‡</sup> Daniel Rauh,<sup>‡</sup> and Stefan A. Laufer<sup>\*,†</sup>

<sup>†</sup>Institute of Pharmacy, Department of Pharmaceutical and Medicinal Chemistry, Eberhard-Karls-University Tübingen, Auf der Morgenstelle 8, 72076 Tübingen, Germany

<sup>‡</sup>Faculty of Chemistry—Chemical Biology, Technische Universität Dortmund, Otto-Hahn-Straße 6, D-44227 Dortmund, Germany

### S Supporting Information

**ABSTRACT:** The p38 MAP kinase is a key player in signaling pathways regulating the biosynthesis of inflammatory cytokines. Small molecule p38 inhibitors suppress the production of these cytokines. Therefore p38 is a promising drug target for novel anti-inflammatory drugs. In this study, we report novel dibenzepinones, dibenzoxepines, and benzosuberones as p38 $\alpha$  MAP kinase inhibitors. Previously reported dibenzepinones and dibenzoxepines were chemically modified by introduction of functional groups or removal of a phenyl ring. This should result in targeting of the hydrophobic region I, the “deep pocket”, and the hinge glycine flip of the kinase. Potent inhibitors with IC<sub>50</sub> values in the single digit nanomolar range (up to 3 nM) were identified. Instead of targeting the “deep pocket” in the DFG-out conformation, interactions with the DFG-motif in the in-conformation could be observed by protein X-ray crystallography.



### INTRODUCTION

Elevated levels of the proinflammatory cytokines tumor necrosis factor- $\alpha$  (TNF- $\alpha$ ) and interleukin-1 $\beta$  (IL-1 $\beta$ ) are implicated in the onset of various autoimmune diseases such as rheumatoid arthritis, Crohn's disease, and psoriasis. Recently the role of p38 in CNS disorders, mainly Alzheimer's disease, was discovered.<sup>1</sup> Clinical and commercial successes of biological agents that neutralize TNF- $\alpha$  (etanercept, infliximab, adalimumab, certolizumabpegol, and golimumab<sup>2–4</sup>) or IL-1 $\beta$  (anakinra<sup>5</sup>) confirmed the central role of these cytokines in the inflammation process. The mitogen-activated protein (MAP) kinase p38 is a key player in signaling pathways regulating the biosynthesis of inflammatory cytokines, including TNF- $\alpha$  and IL-1 $\beta$ , at the translational and transcriptional levels.<sup>6</sup> Small-molecule inhibitors of p38 MAP kinase<sup>7–10</sup> (Figure 1) such as SB203580<sup>11,12</sup> (**1**) can suppress the production of these cytokines. This strategy seems to be promising because a p38 $\gamma$  inhibitor was approved recently for idiopathic pulmonary fibrosis.<sup>13</sup> However, no p38 $\alpha$  MAP kinase inhibitor made it to the market yet, although there are two candidates in clinical trials at the moment: PH-797804<sup>14–17</sup> is in phase III for the treatment of COPD, and BMS-582949<sup>18–20</sup> is in phase II for the treatment of rheumatoid arthritis. Therefore, there is a continuous need for novel orally bioavailable small molecule inhibitors of p38 $\alpha$  MAP kinase.<sup>12,21,22</sup>

We previously reported a novel series of dibenzepinone inhibitors<sup>23</sup> (Figure 2) belonging to the class of so-called linear binders.<sup>8</sup> The phenyl substituent of **3** occupies the hydrophobic region I of the active site and is linked with an amino group to

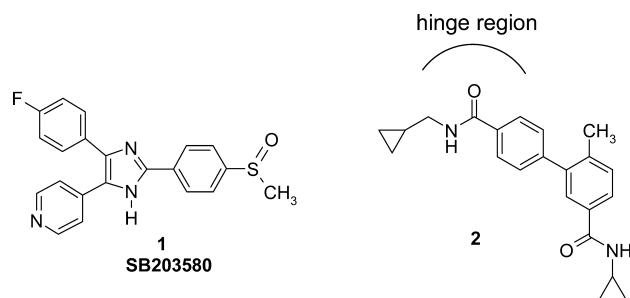


**Figure 1.** Inhibitors of p38 MAP kinase: pyridinylimidazole SB203580<sup>11,12</sup> (**1**) and biphenyl amide (**2**).<sup>15</sup>

the suberone scaffold. The linear constitution of the inhibitor is tolerated due to the relatively small gatekeeper Thr106 in p38 $\alpha$  and contrasts with most other kinases that have more sterically demanding residues at this position. The X-ray cocrystal structure of the dibenzepinone inhibitor **3** in complex with p38 $\alpha$ <sup>24</sup> shows that upon binding of the dibenzepinone inhibitor **3**, the p38 MAP kinase undergoes a Gly110 flip. This glycine flip is a small conformational rearrangement in the hinge region of the p38 $\alpha$  MAP kinase induced by the inhibitor. Gly110, which is able to take a positive torsion angle, is switched about 180°, and **3** binds with its carbonyl oxygen toward the backbone NH of Gly110 and the backbone NH of Met109.

Received: July 4, 2012

Published: August 16, 2012

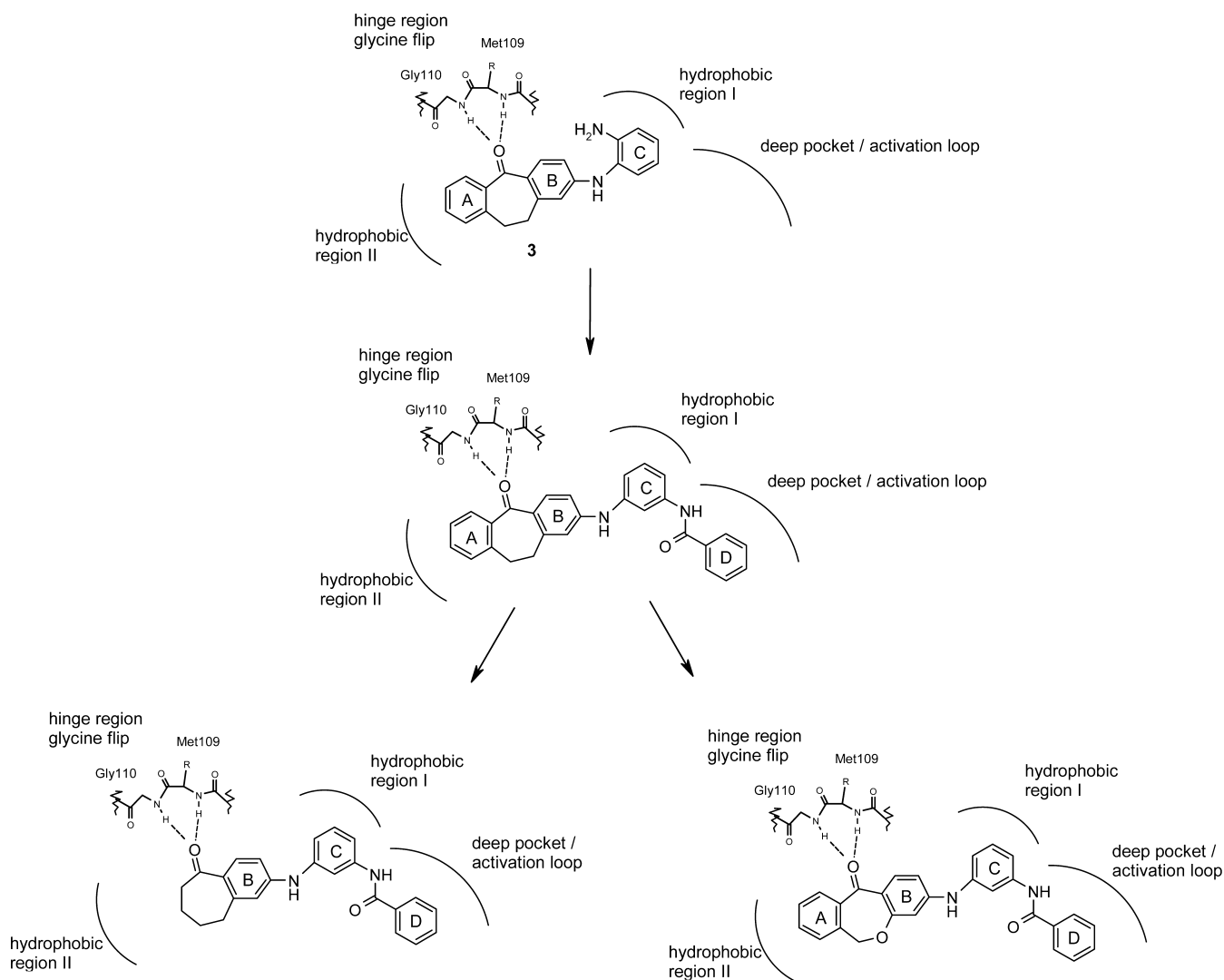
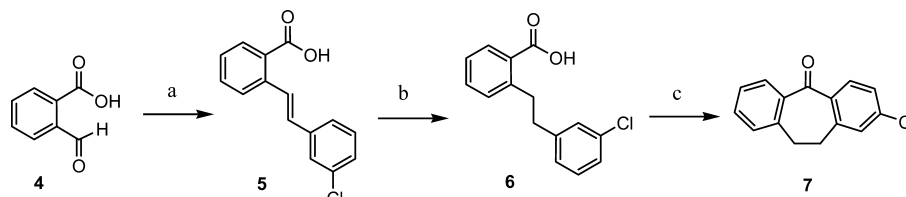


**Figure 2.** Schematic drawing of important interactions between the competitive inhibitor **3** and the ATP binding site of p38 $\alpha$  MAPK.

### Scheme 1. Synthetic Route for the Dibenzepinone Scaffold **7**<sup>a</sup>

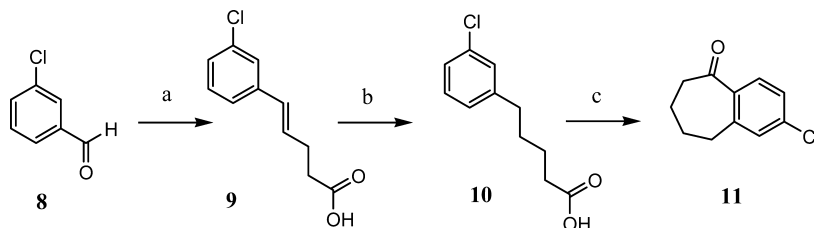


<sup>a</sup>Reagents and conditions: (a) 1. triphenylphosphine, 3-chlorobenzylchloride, methanol, reflux; 2. 2-formylbenzoic acid, sodium methoxide, 0 °C; (b) H<sub>2</sub>, Pd/C, ethyl acetate/acetonitrile, rt; (c) 1. oxalyl chloride, dimethylformamide, dichloromethane, rt; 2. AlCl<sub>3</sub>, dichloromethane, rt.

The glycine flip provides selectivity for p38 $\alpha$  over other kinases with less flexible, nonglycine residues at this position. Only 46 of all 518 kinases are able to perform a glycine flip. Of these 46 kinases, only 3 kinases possess a small threonine as gatekeeper residue in addition to the glycine in the hinge region, which could be utilized to gain further selectivity. In addition, the X-ray structure provided the following information: the A-ring of the dibenzepinone scaffold does not form any relevant interactions with the enzyme and may therefore not be essential for the inhibitory activity. In this study, we report on the synthesis of novel p38 $\alpha$  MAP kinase inhibitors based on SAR from compound **3**.

In a first step (Scheme 2), we focused on the variation of the substitution pattern at the C-ring of the scaffold to target the deep pocket<sup>9</sup> of the p38 $\alpha$  MAP kinase in order to achieve additional interactions with the enzyme, improving the potency of the lead compounds based on data from *in vitro* assays (Tables 1–3).

Second, we removed the A-ring to get a benzosuberone scaffold<sup>25</sup> (Scheme 2) that showed similar inhibitory potency as the dibenzepinone scaffold.<sup>26</sup> Furthermore, we introduced an oxygen to the suberone bridge to obtain the respective dibenzoxepine derivative.<sup>27</sup>

Scheme 2. Synthetic Route for the Benzosuberone Scaffold 11<sup>a</sup>

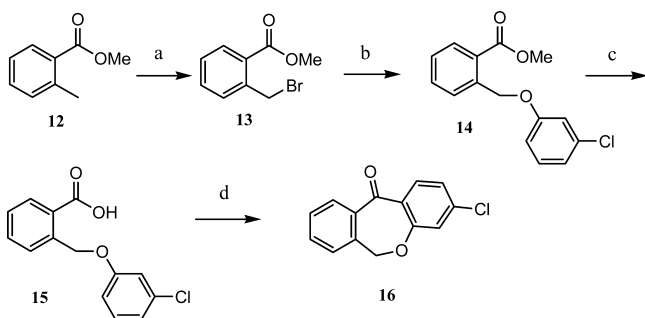
<sup>a</sup>Reagents and conditions: (a) 1. (3-carboxypropyl)triphenylphosphonium bromide, sodium methoxide, methanol, reflux; 2. 3-chlorobenzaldehyde, methanol, reflux; (b) H<sub>2</sub>, Pd/C, ethyl acetate, rt; (c) 1. oxalyl chloride, dimethylformamide, dichloromethane, rt; 2. AlCl<sub>3</sub>, dichloromethane, rt.

## CHEMISTRY

The dibenzepinone scaffold<sup>26</sup> was synthesized as shown in Scheme 1: Wittig reaction of 2-carboxybenzaldehyde and 3-chlorobenzylchloride in the presence of triphenylphosphine and sodium methoxide yields the stilbeno-2-carboxylic acid 5. The ethano linker 6 was obtained by reduction of the alkene 5 with H<sub>2</sub> over Pd/C in ethyl acetate at room temperature. The subsequent ring closure leading to the dibenzepinone 7<sup>26</sup> was best achieved via an intramolecular Friedel-Crafts acylation under standard conditions.

The benzosuberone scaffold was synthesized as shown in Scheme 2.<sup>25</sup> Wittig reaction of 3-chlorobenzaldehyde and (3-carboxypropyl)triphenylphosphonium bromide in the presence of sodium methoxide yields the unsaturated carboxylic acid 9. The saturated carboxylic acid 10 was obtained by reduction of the double bond of 9 with H<sub>2</sub> over Pd/C in ethyl acetate at room temperature. The subsequent ring closure to the benzosuberone 11<sup>25</sup> was best performed by an intramolecular Friedel-Crafts reaction under standard conditions.

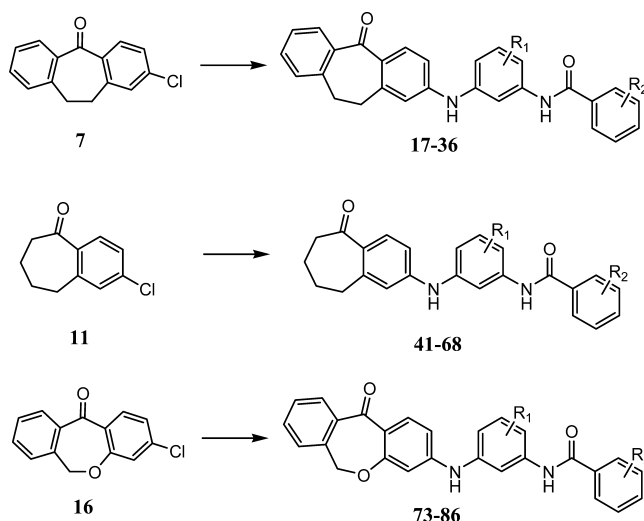
The dibenzoxepine scaffold<sup>27</sup> was synthesized as shown in Scheme 3: A Wohl-Ziegler bromination in carbon tetra-

Scheme 3. Synthetic Route for the Dibenzoxepinone Scaffold 16<sup>a</sup>

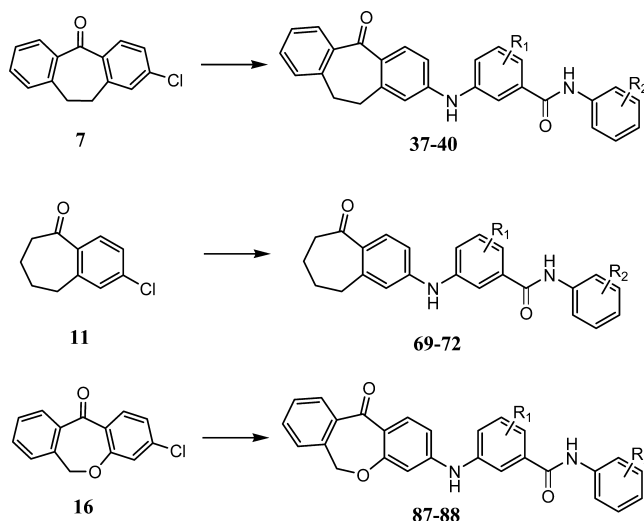
<sup>a</sup>Reagents and conditions: (a) *N*-bromosuccinimide, azobis(isobutyronitrile), carbon tetrachloride, reflux; (b) 1. 3-chlorophenol, K<sub>2</sub>CO<sub>3</sub>, acetone, 50 °C; 2. methyl-2-(bromomethyl)-3-methoxybenzoate, acetone, 70 °C; (c) KOH, methanol, reflux; (d) 1. oxalyl chloride, dimethylformamide, dichloromethane, rt; 2. AlCl<sub>3</sub>, rt.

chloride with *N*-bromo-succinimide and azobis(isobutyronitrile) yields the brominated compound 13. In the next step, compound 14 was obtained by Williamson etherification with 3-chloro-phenol. Then the ester was disrupted to obtain the free carboxylic acid derivative 15. Intramolecular ring closure was achieved via Friedel-Crafts acylation to obtain the dibenzepinone scaffold 16.<sup>27</sup>

Preparation of target compounds 17–40, 41–72, and 73–88 was conducted as shown in Schemes 4 and 5 by reaction of the

Scheme 4. Synthetic Route for Compounds 17–37, 41–68, and 73–86<sup>a</sup>

<sup>a</sup>For the nature of R<sub>1</sub> and R<sub>2</sub>, see Tables 1 and 3.

Scheme 5. Synthetic Route for the Inverse Amide Compounds 37–40, 69–72, and 87–88<sup>a</sup>

<sup>a</sup>For the nature of R<sub>1</sub> and R<sub>2</sub>, see Table 2.

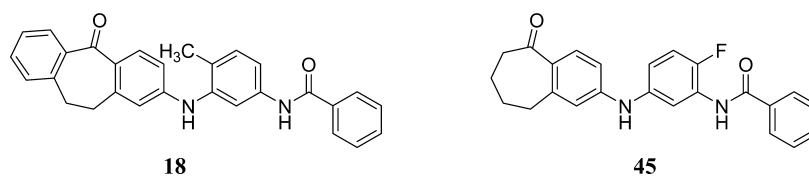


Figure 3. Chemical structure of compounds 18 and 45.

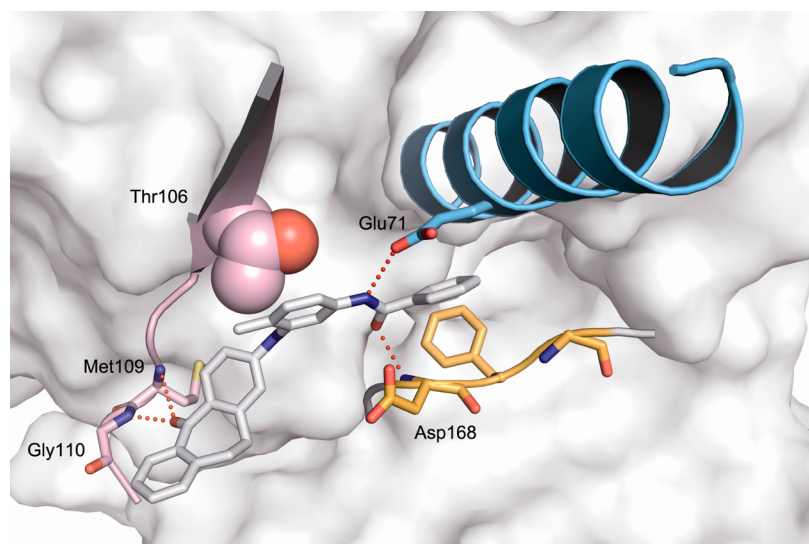


Figure 4. Docking result for compound 18. The hydrogen bonds are indicated as dotted lines.

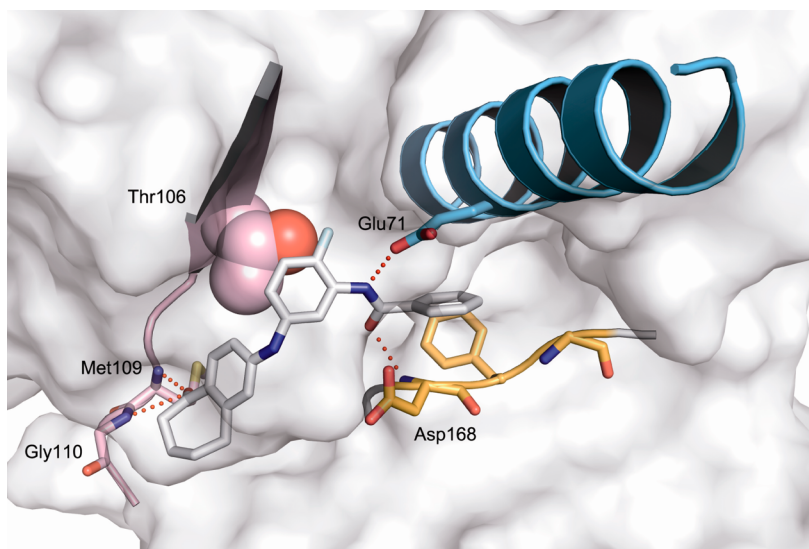


Figure 5. Docking result for compound 45. The hydrogen bonds are indicated as dotted lines.

respective amine with either the dibenzepinone, dibenzoxepine, or benzosuberone scaffold.<sup>29</sup> The respective scaffold 7, 11, or 16 undergoes a palladium-catalyzed amination reaction with the corresponding aryl amine resulting in the final compounds 17–40, 41–72, and 73–88. Synthesis of the final compounds was attained as described above using the respective amines as coupling reagent for the Buchwald–Hartwig reaction.

### ■ BIOLOGICAL TESTING

The inhibitory potencies of compounds 17–40, 41–72, and 73–88 were evaluated using an isolated p38 $\alpha$  enzyme assay,<sup>30</sup> at concentrations ranging from 10  $\mu$ M to 10 nM. The ability of

test compounds to compete with ATP for the ATP binding site of the kinase inversely correlates with the capacity of p38 $\alpha$  MAP kinase to phosphorylate its natural substrate, activating transcription factor 2 (ATF-2), when incubated with ATP and the test compound. SB203580<sup>11,12</sup> was used as a reference compound, and the test was performed with an optimized ATP concentration of 100  $\mu$ M.

### ■ BIOLOGICAL RESULTS AND DISCUSSION

**Docking Studies.** Docking studies conducted with *Glide* from Schrodinger<sup>28</sup> suggested the *meta*-position of the C-ring to be a good site for insertion of a benzamide moiety to achieve

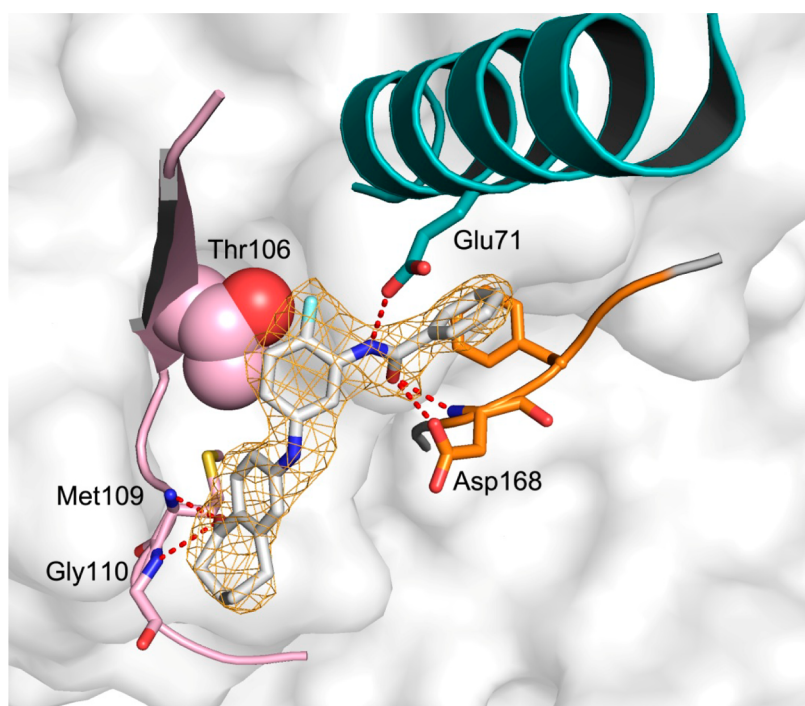


**Figure 6.** Crystal structure of p38 $\alpha$  in complex with 45. The inhibitor binds to the ATP-pocket of p38 $\alpha$  by forming hydrogen bonds (red dotted lines) to the peptide backbone of the hinge region (light pink) (Met109, Gly110) and additional hydrogen bonds to Glu71 in the  $\alpha$ -helix C (blue) and Asp168 in the DFG-motif (orange). The DFG-motif adopts a DFG-in conformation. Electron density map ( $2F_o - F_c$ ) is contoured at  $1\sigma$  using PyMOL (<http://www.pymol.org>).

additional interaction opportunities. The binding mode of compound 18 (Figure 3) in p38 $\alpha$  is shown in Figure 4. Compound 45 (Figure 3) is supposed to interact with p38 in the same way (Figure 5). The predicted binding mode could be verified by X-ray crystallography of p38 $\alpha$  in complex with compound 45 (Figure 6). We intended to target the DFG-out conformation. But the docking results already predicted targeting of the DFG-motif located in the activation loop.

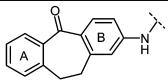
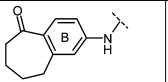
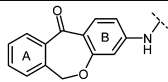
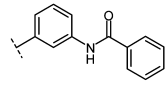
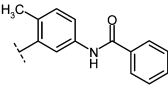
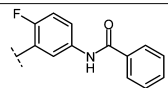
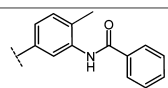
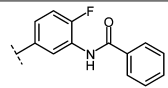
#### Variation of the Substitution Pattern of the C-Ring.

Because the C-ring addresses the hydrophobic region I to some extent, we chose fluoro substituents at the 2- or 4-position (compounds 19, 21, 43, 45, 75, and 77) since compounds with such a substitution pattern showed favorable results in our previously published series.<sup>23</sup> For comparison, we further attached a methyl group at the 2- or 4-position (compounds 18, 20, 42, 44, 74, and 76). For the biphenyl amide series, exemplified by 2 (Figure 1), the methyl group on the toluene ring is one of the key requirements for p38 $\alpha$  inhibitory activity.<sup>31</sup> An analogue of 2 that lacks the 4-methyl group (also called the “magic methyl” group)<sup>32,33</sup> shows a nearly 100-fold decreased p38 $\alpha$  activity.<sup>31</sup> Other p38 $\alpha$ -inhibitors such as the 2-tolyl-(1,2,3-triazol-1-yl-4-carboxamide) inhibitors from Boehringer Ingelheim<sup>34</sup> and the pyrrolo[2,1-*f*][1,2,4]triazine inhibitors from Bristol-Myers Squibb<sup>35</sup> also bear a methyl group. In the dibenzepinone series (Table 1), the replacement of hydrogen (compound 17) by a methyl group (compound 18) did not increase p38 $\alpha$  activity, because compound 17 already showed an IC<sub>50</sub> value of 36 nM. In fact, we found another relevant position; compound 20, bearing a methyl substituent at the 2-position, showed an IC<sub>50</sub> value of 10 nM, which resulted in a 4-fold higher inhibitory activity compared with reference 3. Compound 21, carrying a fluoro substituent in 2-position, showed even higher activity against p38 $\alpha$  MAP

kinase resulting in an IC<sub>50</sub> value of 5 nM. However, the evaluation of the benzosuberone series (Table 1) showed the inverse effect: replacing the hydrogen at position 2 of compound 41 with either fluorine (compound 45) or methyl (compound 44), which proved to be important for the dibenzepinone series, showed no effect or even decreased the activity nearly 4-fold. For this series, we could confirm the “magic” position described in the literature: substituting the hydrogen at position 4 increased the inhibitory potency nearly three times. This resulted in IC<sub>50</sub> values as low as 12 nM for compound 43, bearing a fluoro substituent at position 4. However, the “magic methyl” effect is not as pronounced as described in the literature, which could be explained by the different binding mode of the compounds. As described below, they do not interact with the deep pocket but with the activation loop. In the dibenzoxepine series, position 2 as well as position 4 substituted derivatives (compounds 74–77) showed an increased inhibitory activity, compared with compound 73, up to an IC<sub>50</sub> value of 17 nM for compound 74.

**Inverse Amide.** In order to verify whether the regiochemistry of the amide is important for the inhibitory activity, we synthesized compounds 37–40, 69–72, and 87–88 (Table 2). Kinase assay data showed that the inverse amide moiety results in much poorer inhibitory activity (compare 17, 41, and 73 with 37, 69, and 87). Thus, the variety of the amide plays a crucial role in the interaction between inhibitor and p38 $\alpha$ . Investigators from GlaxoSmithKline obtained opposite results: compared with compound 2, the compound modified with another type of amide (Figure 7) showed poorer inhibitory activity, with IC<sub>50</sub> values of 2.3  $\mu$ M, compared with 0.075  $\mu$ M for 2. Additional studies with other p38 $\alpha$  inhibitors such as 2-tolyl-(1,2,3-triazol-1-yl-4-carboxamide) inhibitors from Boehringer Ingelheim<sup>34</sup> and pyrrolo[2,1-*f*][1,2,4]triazine inhibitors

Table 1. Evaluation of p38 $\alpha$  MAP Kinase Activity for Compounds 17–21, 41–45, and 73–77 Based on the Rate of Phosphorylation of ATF-2 (Activation Transcription Factor 2) Using an Isolated p38 $\alpha$  Assay<sup>13c</sup>

R <sub>1</sub> <sup>c</sup>						
	compd.	p38 $\alpha$ [ $\mu$ M] <sup>a</sup> IC <sub>50</sub> $\pm$ SEM	compd.	p38 $\alpha$ [ $\mu$ M] <sup>a</sup> IC <sub>50</sub> $\pm$ SEM	compd.	p38 $\alpha$ [ $\mu$ M] <sup>a</sup> IC <sub>50</sub> $\pm$ SEM
	<b>3</b>	0.05 $\pm$ 0.01				
	<b>17</b>	0.036 $\pm$ 0.012	<b>41</b>	0.037 $\pm$ 0.005	<b>73</b>	0.055 $\pm$ 0.010
	<b>18</b>	0.035 $\pm$ 0.009	<b>42</b>	0.014 $\pm$ 0.004	<b>74</b>	0.017 $\pm$ 0.003
	<b>19</b>	0.014 $\pm$ 0.002	<b>43</b>	0.012 $\pm$ 0.002	<b>75</b>	0.024 $\pm$ 0.001
	<b>20</b>	0.010 $\pm$ 0.002	<b>44</b>	0.12 $\pm$ 0.04	<b>76</b>	0.025 $\pm$ 0.002
	<b>21</b>	0.005 $\pm$ 0.002	<b>45</b>	0.035 $\pm$ 0.002	<b>77</b>	0.020 $\pm$ 0.017

<sup>a</sup>Mean  $\pm$  SD of three trials. <sup>b</sup>Substituents are numbered as shown for presentational uniformity; see Experimental Section and Supporting Information for correct numbering of substituents. <sup>c</sup>IC<sub>50</sub> of SB203580 = 0.037  $\pm$  0.003  $\mu$ M ( $n$  = 25).

from Bristol-Myers Squibb<sup>35</sup> have reported compounds with only one type of amide. The structures of inhibitors from Bristol-Myers Squibb<sup>35</sup> are comparable to our most favorable substituent. In comparison to our most successful compounds, Boehringer Ingelheim<sup>34</sup> reported inhibitors with the inverse structure of the amide. This could be explained by a slightly different position of the inhibitor in complex with the enzyme due to either one or two hydrogen bonds between inhibitor and hinge region.

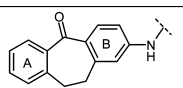
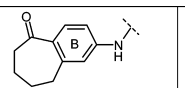
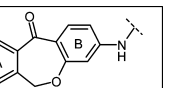
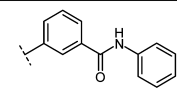
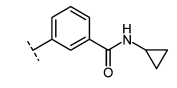
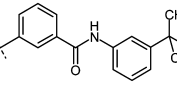
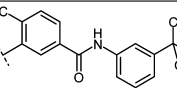
**Variation of the D-Ring.** Compounds **22** and **46–48**, bearing a *tert*-butyl moiety in the *para*-position of the D-ring, were not tolerated as well as the extended acetic and propionic acid moieties (**29–30** and **58–61**), presumably due to steric hindrance (Table 3). This could also explain the decreased activity of compounds **50** and **52** in comparison to compound **24**.

Based on docking studies, we chose to vary the *meta*-position in the substitution pattern of the D-ring of the dibenzepinone, the dibenzoxepine, and the benzosuberone scaffold. Compounds with various substituents **23**, **49**, and **78**, **24** and **51**, and **25–28**, **53–57** and **79** and **80** were tested in the enzyme assay. Besides compound **26**, compounds **24** and **28** resulted in comparable or even better inhibitory activity than the unsubstituted compound **17**. The introduction of a methoxy group (compound **24**) in the *meta*-position improved the

inhibitory activity by about 3-fold. This outcome could be due to a direct interaction between the methoxy group and the enzyme. Interestingly, the fluoro substituent in the *para*-position (**26**) yielded a 10-fold higher inhibitory activity compared with the *meta*-position (**25**). Compound **26** was similar in inhibitory activity in comparison to compound **17** with the unsubstituted D-ring. Unexpectedly, this structure–activity relationship only applies to the dibenzepinone scaffold, not to the benzosuberone scaffold. The comparison of compound **51** bearing the *meta*-methoxy group with the unsubstituted compound **41** shows a 4-fold decreased inhibitory activity. Compound **52** with a *para*-methoxy substituent showed the best activity in the methoxy series with an IC<sub>50</sub> of 84 nM. Combination of the 2-fluoro substituent on the C-ring with the *meta*-fluoro substituent on the D-ring resulted in a good inhibitory activity (compound **54**, IC<sub>50</sub> = 40 nM). In the dibenzoxepine series, two substituents in the *meta*-position with good inhibitory activity could be identified: compound **78** with a *meta*-methyl substituent (IC<sub>50</sub> = 15 nM) and compound **80** with a *meta*-morpholino substituent (IC<sub>50</sub> = 30 nM). These results indicate that the three scaffolds are not comparable at all regarding their inhibitory effects.

Results of the replacement of the phenyl by various heterocycles are summarized in Table 3. The aromatic heterocycles (**32–36**, **63–67**, and **81–85**) seem to be

**Table 2.** Evaluation of p38 $\alpha$  MAP Kinase Activity Based on the Rate of Phosphorylation of ATF-2 Using an Isolated p38 $\alpha$  Assay<sup>13b</sup>

R						
	compd.	p38 $\alpha$ [ $\mu$ M] <sup>a</sup> IC <sub>50</sub> $\pm$ SEM	compd.	p38 $\alpha$ [ $\mu$ M] <sup>a</sup> IC <sub>50</sub> $\pm$ SEM	compd.	p38 $\alpha$ [ $\mu$ M] <sup>a</sup> IC <sub>50</sub> $\pm$ SEM
	<b>3</b>	0.05 $\pm$ 0.01				
	<b>37</b>	1.2 $\pm$ 0.1	<b>69</b>	6.2 $\pm$ 1.3	<b>87</b>	3.8 $\pm$ 1.0
	<b>38</b>	0.20 $\pm$ 0.02	<b>70</b>	4.8 $\pm$ 1.7	<b>88</b>	26% @ 10 $\mu$ M
	<b>39</b>	2.0 $\pm$ 0.6	<b>71</b>	4.7 $\pm$ 0.3	-	-
	<b>40</b>	1.5 $\pm$ 0.2	<b>72</b>	0.10 $\pm$ 0.01	-	-

<sup>a</sup>Mean  $\pm$  SD of three trials. <sup>b</sup>IC<sub>50</sub> of SB203580 = 0.037  $\pm$  0.003  $\mu$ M ( $n$  = 25).

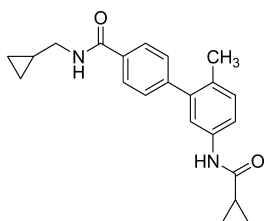


**Figure 7.** Inverse amide compound from GlaxoSmithKline.<sup>31</sup>

advantageous compared with the cyclopropyl moiety (**31** and **62**). The location of the heteroatom in *meta*-position (**32–36**, **63–67**, and **81–85**) was more favorable than in *ortho*-position. This effect confirms the result of compound **24**: the introduction of a hydrogen bond acceptor in the *meta*-position ameliorates the inhibitory effect, probably due to an additional interaction opportunity. Interestingly, the location of the heteroatom plays a crucial role for the benzosuberone scaffold as well. At first sight, there seems to be no explanation for the poor effect of the *meta*-substituents compared with the promising results from the heterocycles.

However, all the differences in the structure–activity relationships described above cannot be explained by the docking results.

Finally, the combination of the best substituents of the C-ring and the best variation of the D-ring resulted in compound **83** with a low nanomolar inhibitory activity (IC<sub>50</sub> = 10 nM) and in compound **34**, where the combination of the best substitution pattern resulted in an increase of potency; the compound showed an IC<sub>50</sub> of 4 nM. The most active

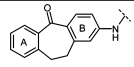
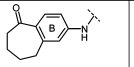
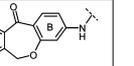
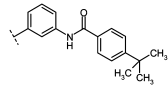
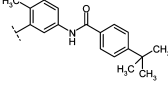
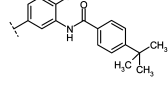
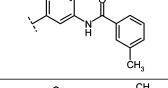
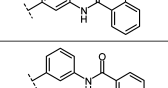
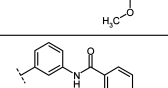
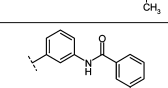
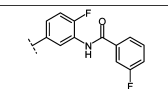
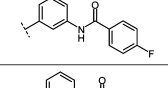
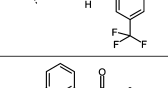
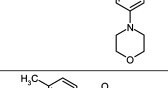
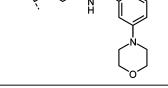
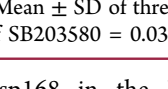
compound of this series is compound **68**, which combines two substituents on the C-ring with the 3-thiophene as replacement for the phenyl ring D. This results in an excellent inhibitory activity of 3 nM.

**Kinase Selectivity Profiling.** As we removed the A-ring of the dibenzepinone scaffold and introduced amide residues to the C-ring, it was necessary to confirm that this did not lead to a loss of selectivity in comparison to the highly selective reference compound. Therefore selectivity profiling of compound **45** against a panel of 333 kinases was performed.<sup>36</sup> At a concentration of 10  $\mu$ M, only 6 out of 333 kinases were inhibited >50%: CAMK2D, CK1- $\delta$ , CK1- $\epsilon$ , SLK, p38 $\alpha$ , and p38 $\beta$ . However, only p38 $\alpha$  and p38 $\beta$  were inhibited substantially. This leads to the result that the loss of the A-ring and the introduction of amide moieties do not affect the selectivity.

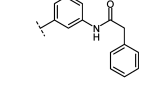
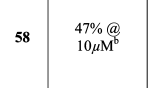
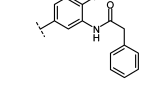
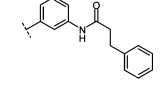
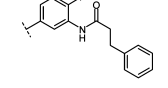
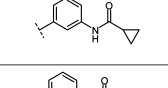
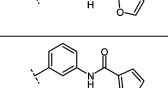
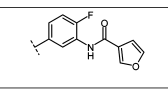
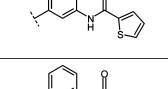
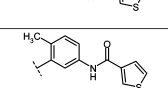
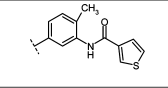
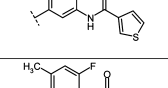
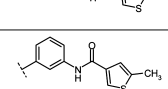
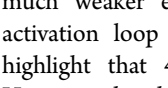
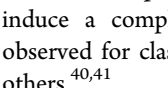
**Physicochemical Properties.** The physicochemical properties of all the compounds are not perfect: the log *P* is rather high with values over 5. This may result in some drawbacks such as low solubility, which is a common problem of this amide series. Thus there is further work necessary to improve the ADME properties of the amide compounds.

**X-ray Crystallography.** The binding mode of compound **45** in complex with p38 $\alpha$  MAP kinase (Figure 6) was determined by protein X-ray crystallography (Table 4). The central carbonyl oxygen of the benzosuberone scaffold induces the expected glycine flip in the hinge region and forms two hydrogen bonds with the backbone of Met109 and Gly110. In addition, polar interactions can be observed between the amide NH and Glu71 ( $\alpha$ -helix C) and the amide carbonyl oxygen and

**Table 3. Evaluation of p38 $\alpha$  MAP Kinase Activity for Compounds 22–36, 46–68, and 78–86 Based on the Rate of Phosphorylation of ATF-2 Using an Isolated p38 $\alpha$  Assay<sup>13c</sup>**

R						
	compd.	p38 $\alpha$ [ $\mu$ M] <sup>a</sup> IC <sub>50</sub> $\pm$ SEM	compd.	p38 $\alpha$ [ $\mu$ M] <sup>a</sup> IC <sub>50</sub> $\pm$ SEM	compd.	p38 $\alpha$ [ $\mu$ M] <sup>a</sup> IC <sub>50</sub> $\pm$ SEM
	<b>3</b>	0.05 $\pm$ 0.01				
	<b>22</b>	43% @10 $\mu$ M <sup>b</sup>	<b>46</b>	39% @ 10 $\mu$ M <sup>b</sup>	-	-
	-	-	<b>47</b>	2.7 $\pm$ 0.9	-	-
	-	-	<b>48</b>	1.6 $\pm$ 0.4	-	-
	<b>23</b>	0.35 $\pm$ 0.03	<b>49</b>	0.85 $\pm$ 0.13	<b>78</b>	0.015 $\pm$ 0.003
	-	-	<b>50</b>	0.22 $\pm$ 0.03	-	-
	<b>24</b>	0.013 $\pm$ 0.003	<b>51</b>	0.16 $\pm$ 0.04	-	-
	-	-	<b>52</b>	0.084 $\pm$ 0.027	-	-
	<b>25</b>	0.30 $\pm$ 0.10	<b>53</b>	0.21 $\pm$ 0.02	<b>79</b>	0.18 $\pm$ 0.005
	-	-	<b>54</b>	0.040 $\pm$ 0.009	-	-
	<b>26</b>	0.040 $\pm$ 0.003	<b>55</b>	0.13 $\pm$ 0.017	-	-
	<b>27</b>	0.97 $\pm$ 0.05	<b>56</b>	4.8 $\pm$ 0.2	-	-
	-	-	<b>57</b>	0.13 $\pm$ 0.09	<b>80</b>	0.030 $\pm$ 0.002
	<b>28</b>	0.042 $\pm$ 0.001	-	-	-	-

R						
	compd.	p38 $\alpha$ [ $\mu$ M] <sup>a</sup> IC <sub>50</sub> $\pm$ SEM	compd.	p38 $\alpha$ [ $\mu$ M] <sup>a</sup> IC <sub>50</sub> $\pm$ SEM	compd.	p38 $\alpha$ [ $\mu$ M] <sup>a</sup> IC <sub>50</sub> $\pm$ SEM
	<b>29</b>	3.1 $\pm$ 0.3	<b>58</b>	47% @ 10 $\mu$ M <sup>b</sup>	-	-
	-	-	<b>59</b>	3.3 $\pm$ 0.3	-	-
	<b>30</b>	4.3 $\pm$ 0.6	<b>60</b>	44% @ 10 $\mu$ M <sup>b</sup>	-	-
	-	-	<b>61</b>	4.4 $\pm$ 0.4	-	-
	<b>31</b>	0.083 $\pm$ 0.002	<b>62</b>	0.99 $\pm$ 0.28	-	-
	<b>32</b>	0.027 $\pm$ 0.001	<b>63</b>	0.22 $\pm$ 0.08	-	-
	<b>33</b>	0.009 $\pm$ 0.002	-	-	<b>81</b>	0.040 $\pm$ 0.004
	<b>34</b>	0.004 $\pm$ 0.001	<b>64</b>	0.032 $\pm$ 0.002	-	-
	<b>35</b>	0.029 $\pm$ 0.005	-	-	-	-
	<b>36</b>	0.010 $\pm$ 0.001	<b>65</b>	0.012 $\pm$ 0.001	<b>82</b>	0.020 $\pm$ 0.001
	-	-	<b>66</b>	0.027 $\pm$ 0.001	-	-
	-	-	-	-	<b>83</b>	0.011 $\pm$ 0.001
	-	-	<b>67</b>	0.017 $\pm$ 0.002	<b>84</b>	0.010 $\pm$ 0.001
	-	-	<b>68</b>	0.003 $\pm$ 0.004	<b>85</b>	0.012 $\pm$ 0.002
	-	-	-	-	<b>86</b>	6.8 $\pm$ 0.545

<sup>a</sup>Mean  $\pm$  SD of three trials. <sup>b</sup>% Inhibition at 10  $\mu$ M. See Experimental Section/Supporting Information for correct numbering of substituents. <sup>c</sup>IC<sub>50</sub> of SB203580 = 0.037  $\pm$  0.003  $\mu$ M ( $n$  = 25).

Asp168 in the DFG-motif of the activation loop. The phenylamino moiety of the inhibitor occupies the hydrophobic region I of the kinase to some extent, and the kinase adopts the active DFG-in conformation as observed for common type I inhibitors like Scio-496.<sup>37,38</sup> Interestingly, some residual electron density around the flexible activation loop indicates partial existence of the DFG-out conformation although to a

much weaker extent. Partial or mixed occupancies in the activation loop of protein kinases are not uncommon and highlight that **45** can bind to both DFG conformations. However, the phenylamino moiety of **45** is not bulky enough to induce a complete shift to the DFG-out conformation as observed for classic type II inhibitors such as BIRB-796<sup>39</sup> and others.<sup>40,41</sup>

**Table 4. Data Collection and Refinement Statistics for p38 $\alpha$  with Compound 45 (3UVP)**

Data Collection	
space group	$P2_12_12_1$
cell dimensions	
$a, b, c$ (Å)	64.00, 68.80, 74.80
$\alpha, \beta, \gamma$ (deg)	90.00, 90.00, 90.00
resolution (Å)	50.0–2.4 (2.50–2.40) <sup>a</sup>
$R_{\text{sym}}$ or $R_{\text{merge}}$ (%)	9.3 (41.2)
$I/\sigma I$	15.43 (3.95)
completeness (%)	99.8 (99.6)
redundancy	5.19 (4.59)
Refinement	
resolution (Å)	48.63–2.40
no. reflns	13405
$R_{\text{work}}/R_{\text{free}}$	21.5/29.7
no. atoms	
protein	2692
ligand/ion	69
water	50
B-factors	
protein	37.2
ligand/ion	37.3
water	38.3
rms deviations	
bond lengths (Å)	0.014
bond angles (deg)	1.488
structure (PDB-ID code)	p38 $\alpha$ with 45 (3UVP)
wavelength (Å)	0.978 600
temperature	90 K
X-ray source	SLS X10SA
Ramachandran plot	
residues in most favored regions	87.7%
residues in additional allowed regions	11.3%
residues in generously allowed regions	1.0%
residues in disallowed regions	0.0%

<sup>a</sup>Diffraction data from one crystal was used to determine the complex structure. Values in parentheses refer to the highest resolution shell.

## CONCLUSION

The removal of the A-ring had no substantial effect on the inhibitory activity of p38 MAP kinase because the respective benzosuberone derivatives showed comparable inhibitory effects to the dibenzepinone and dibenzoxepine scaffolds.

By variation of the phenylamino moiety of the three scaffolds and introduction of a substituted benzamide moiety that afforded further interaction opportunities, we obtained compounds with improved inhibitory activity. As suggested by docking studies, the *meta*-position of the ring D proved to be suitable for the introduction of further substituents. The binding mode of compound 45 could be confirmed by X-ray crystallography: compound 45 induces the hinge glycine flip and binds to the activation loop. Compared with the lead structure 3, the inhibitory potency could be increased by about 10-fold down to the low nanomolar range as exemplified by compounds 21, 34, 68, and 84 with IC<sub>50</sub> values of 5, 4, 3, and 10 nM, respectively.

## EXPERIMENTAL SECTION

All commercially available reagents and solvents were used without further purification. Melting points were determined with a Büchi melting point device, model B-545, and were thermodynamically

corrected. <sup>1</sup>H NMR (200/400 MHz) and <sup>13</sup>C NMR (50/100 MHz) spectra were recorded on a Bruker Avance 200 and a Bruker Avance 400. Chemical shifts are reported in ppm from the solvent resonance. IR data were determined on a Perkin-Elmer Spectrum One spectrometer (ATR technique). Flash chromatography was performed using a LaFlash system (VWR) with Merck silica gel (25–40  $\mu$ m). The purity of the final compounds was determined by HPLC (Merck Hitachi L-6200 intelligent pump, Merck Hitachi AS-2000 autosampler, Merck Hitachi L-4250 UV–vis detector) using a LiChrospher C18 column (5  $\mu$ m), employing a gradient of 0.01 M KH<sub>2</sub>PO<sub>4</sub> (pH 2.3) and methanol as solvent system with a flow rate of 1.0 mL/min and detection at 254 nm. Mass spectra were run on a Hewlett-Packard HP 6890 series GC-system equipped with a HP-5MS capillary column (0.25  $\mu$ m film thickness 30 m  $\times$  0.25 mm) and a Hewlett-Packard HP 5973 mass selective detector (70 eV). HRMS (EI) (electron impact–high-resolution mass spectroscopy) data were obtained from the department for mass spectrometry, Institute of Organic Chemistry, Eberhard-Karls-University Tübingen. All compounds were >95% pure. See Supporting Information for details.

**Amination Reaction with the Dibenzepinone Scaffold (General Procedure A).** A mixture of 2.1 mmol aryl chloride, 2.1 mmol amine, 4.6 mmol of the corresponding base, 90 mg (0.19 mmol) of 2-(dicyclohexylphosphino)-2',4',6'-triisopropylbiphenyl and 20 mg (0.09 mmol) of Pd(OAc)<sub>2</sub> in 2 mL of absolute *tert*-butanol and 8 mL of absolute toluol was stirred at 90 °C under an atmosphere of argon. For compounds 17, 25, and 37, Cs<sub>2</sub>CO<sub>3</sub> was used as base, for compounds 20, 23, 27, 31, 33, 34, 35, 39, and 40, KO<sup>*t*</sup>-Bu was used as base, and for the other compounds, NaO<sup>*t*</sup>-Bu was used. When the reaction was completed, the mixture was allowed to cool to room temperature, diluted with water, and extracted with ethyl acetate. The extracts were combined, washed with saturated saline solution, and then dried over Na<sub>2</sub>SO<sub>4</sub>. The solvent was removed under vacuum, and the residue was purified by flash chromatography (SiO<sub>2</sub> 60, *n*-hexane/ethyl acetate).

**Amination Reaction with the Benzosuberone Scaffold (General Procedure B).** A mixture of 1.85 mmol of aryl chloride, 1.85 mmol of amine, 22 mmol of the corresponding base, 110 mg (0.2 mmol) of 2-(dicyclohexylphosphino)-2',4',6'-triisopropylbiphenyl, and 20 mg (0.09 mmol) of Pd(OAc)<sub>2</sub> in 2 mL of absolute *tert*-butanol and 10 mL of absolute toluol was stirred at 90 °C under an atmosphere of argon. For compounds 42, 45, 46, 47, 48, 53, 54, and 71, NaO<sup>*t*</sup>-Bu was used as base, and for the other compounds, KO<sup>*t*</sup>-Bu was used. When the reaction was completed, the mixture was allowed to cool to room temperature. It was diluted with water and subsequently extracted with diethyl ether. The extracts were combined, washed with saturated saline solution, and afterwards dried over Na<sub>2</sub>SO<sub>4</sub>. The solvent was removed under vacuum, and the residue was purified by flash chromatography (SiO<sub>2</sub> 60, *n*-hexane/ethyl acetate).

**Amination Reaction with the Dibenzoxepinone Scaffold (General Procedure C).** A mixture of 200 mg (0.81 mmol) of 3-chloro-dibenzo[*b,e*]oxepin-11(6*H*)-one, 700 mg of Cs<sub>2</sub>CO<sub>3</sub> (2.14 mmol), 250 mg (1.18 mmol) of amide, 100 mg (0.21 mmol) of 2-(dicyclohexylphosphino)-2',4',6'-triisopropylbiphenyl, 20 mg (0.09 mmol) of Pd(OAc)<sub>2</sub>, 10 mL of absolute 1,4-dioxane and 2 mL of absolute *tert*-butanol was heated under argon to 110 °C and stirred for 3 h. When the reaction was completed, the mixture was allowed to cool to room temperature. Then the solvents were evaporated, and the residue was purified by flash chromatography (SiO<sub>2</sub> 60, dichloromethane/ethanol).

**2-(3-Chlorophenethenyl)benzoic acid (5).** Triphenylphosphine (15.3 g, 58 mmol) was diluted in 100 mL of methanol, 9.4 g (58 mmol) of 3-chlorobenzylchloride (diluted in 50 mL of methanol) was added dropwise to the stirred solution, and the solution was heated under reflux for 2 h. The reaction mixture was cooled to 0 °C, and 8.7 g (58 mmol) of 2-formylbenzoic acid was added. At 0 °C, 28.0 g (145 mmol) of sodium methoxide (28% in methanol) was added dropwise over a period of 45 min. Afterwards the solution was stirred for 3 h at 0 °C. The reaction mixture was poured onto a stirred mixture of 75 g of ice and 175 mL of H<sub>2</sub>O, filtered, and washed several times with H<sub>2</sub>O, and the combined aqueous phases were subsequently washed several

times with dichloromethane. The product was precipitated by acidification of the aqueous extract. Mp: 125 °C. IR (ATR): 2816, 2648, 2530, 1673, 1567, 1416, 1305, 1273, 799, 784, 715 cm<sup>-1</sup>. <sup>1</sup>H NMR (DMSO-*d*<sub>6</sub>) δ in ppm: 6.59 (d, 1H, *J* = 12.3 Hz), 6.91–6.94 (m, 1H), 7.03–7.19 (m, 5 H), 7.35–7.42 (m, 2H).

**2-(3-Chlorophenethyl)benzoic acid (6).** Five grams (19 mmol) of **5** was dissolved in a mixture of 75 mL of ethyl acetate and 75 mL of acetonitrile, and 100 mg of palladium on activated carbon was added. The mixture was stirred under hydrogen atmosphere for 5 h at room temperature. The mixture was filtered, and the solvent was removed in vacuo. Mp: 220 °C. IR (ATR): 2930, 1697, 1578, 1490, 1442, 1381, 1261, 1139, 1080, 988, 741 cm<sup>-1</sup>. <sup>1</sup>H NMR (DMSO-*d*<sub>6</sub>) δ in ppm: 2.78–2.86 (m, 2 H), 3.13–3.21 (m, 2 H), 7.15–7.33 (m, 5 H), 7.43 (d, 1 H, *J* = 7.2 Hz), 7.83 (d, 1 H, *J* = 8.0 Hz), 12.95 (s, 1 H).

**2-Chloro-10,11-dihydrodibenzo[*a,d*]cyclohepten-5-one (7).** Five grams (20 mmol) of **6** was dissolved in 150 mL of dichloromethane, and then 2.54 g (20 mmol) of oxalyl chloride and catalytic amounts of dimethylformamide were added dropwise, and the mixture was stirred at room temperature for 1 h under argon atmosphere. The mixture was added to a suspension of 3.4 g (30 mmol) of AlCl<sub>3</sub> in dichloromethane and stirred for 4 h at room temperature and afterwards poured onto ice, extracted with dichloromethane, washed with NaOH and H<sub>2</sub>O, and dried over Na<sub>2</sub>SO<sub>4</sub>, and the solvent was removed in vacuo. Mp: 69 °C. IR (ATR): 2942–2847, 1767, 1634, 1581, 1283, 1242, 1186, 1105, 940, 911, 829, 760, 685 cm<sup>-1</sup>. <sup>1</sup>H NMR (DMSO-*d*<sub>6</sub>) δ in ppm: 3.10 (s, 4 H), 7.27–7.49 (m, 5 H), 7.83–7.87 (m, 2 H).

**5-(3-Chlorophenyl)pent-4-enoic acid (9).** To a suspension of 13.91 g (32.4 mmol) of (3-carboxypropyl)triphenylphosphonium bromide in anhydrous methanol, 10.80 g (60 mmol) of 30% sodium methoxide in methanol was added. The mixture was heated to reflux under argon atmosphere for 1 h, and after that a solution of 3.94 g (28 mmol) of 3-chlorobenzaldehyde in methanol was dropwise added. The resulting mixture was stirred for further 6 h, allowed to cool to room temperature, poured onto ice, and extracted with diethyl ether. Subsequently, the aqueous solution was acidified with concentrated HCl and extracted three times with diethyl ether. The organic layer was washed with H<sub>2</sub>O, dried over Na<sub>2</sub>SO<sub>4</sub>, and concentrated in vacuo. The residue was purified using flash chromatography (petrol ether/ethyl acetate, 1:1) to afford a yellowish oil. IR (ATR): 2941, 2866, 1727, 1675, 1589, 1282, 1259, 1091, 964, 824, 785, 751 cm<sup>-1</sup>. HPLC: 7.34 min (98.8%). <sup>1</sup>H NMR (DMSO-*d*<sub>6</sub>) δ in ppm: 2.38 (s, 4 H), 6.38–6.39 (m, 2 H), 7.24–7.29 (m, 4 H).

**5-(3-Chlorophenyl)pentanoic acid (10).** Four grams (19 mmol) of **9** was dissolved in 100 mL of ethyl acetate, and 400 mg of palladium on activated carbon was added. The resulting suspension was stirred under hydrogen atmosphere for 5 h at room temperature. Afterwards, the mixture was filtered and concentrated in vacuo to afford an oil. <sup>1</sup>H NMR (DMSO-*d*<sub>6</sub>) δ in ppm: 1.45–1.57 (m, 4 H), 2.18–2.28 (m, 2 H), 3.85 (s, 2 H), 7.11–7.24 (m, 4 H).

**2-Chloro-6,7,8,9-tetrahydrobenzocyclohepten-5-one (11).** Three grams (14 mmol) of **10** was dissolved in 20 mL of dichloromethane, 1.77 g (14 mmol) of oxalyl chloride and catalytic amounts of dimethylformamide were added dropwise, and the mixture was stirred at room temperature for 1 h under argon atmosphere. The mixture was added to a suspension of 9.0 g (367 mmol) of AlCl<sub>3</sub> in dichloromethane and stirred for 4 h at room temperature and then poured onto ice, extracted with dichloromethane, washed with NaOH and H<sub>2</sub>O, and dried over Na<sub>2</sub>SO<sub>4</sub>, and the solvent removed in vacuo. The extract was further purified by flash chromatography (*n*-hexane/ethyl acetate, 9:1) to obtain a yellowish oil. IR (ATR): 2920, 2612, 1703, 1592, 1575, 1472, 1419, 1288, 1255, 1203, 1076, 962, 887, 713 cm<sup>-1</sup>. HPLC: 7.17 min (99.1%). <sup>1</sup>H NMR (DMSO-*d*<sub>6</sub>) δ in ppm: 1.64–1.80 (m, 4 H), 2.67 (t, 2 H, *J*<sub>1</sub> = 5.56 Hz, *J*<sub>2</sub> = 6.3 Hz), 2.92 (t, 2 H, *J*<sub>1</sub> = 6.7 Hz, *J*<sub>2</sub> = 5.56 Hz), 7.40–7.42 (m, 2 H), 7.56 (d, 1H, *J* = 8.2 Hz). <sup>13</sup>C NMR (DMSO-*d*<sub>6</sub>) δ in ppm: 20.5, 24.8, 31.4, 40.7, 126.9, 129.8, 130.4, 137.1, 137.4, 144.1, 204.2.

**Methyl-2-(bromomethyl)benzoate (13).** Four grams (26.40 mmol) of methyl-2-methylbenzoate and 4.74 g (26.40 mmol) of *N*-bromosuccinimide were dissolved in tetrachloromethane and heated to

reflux. Then 100 mg (0.60 mmol) of azobis(isobutyronitrile) was added. After the reaction was completed, the solid was filtered, and the organic phase was evaporated in vacuo to obtain a yellow oil. <sup>1</sup>H NMR (DMSO-*d*<sub>6</sub>) δ in ppm: 3.87 (s, 3 H, -OCH<sub>3</sub>), 5.01 (s, 2 H, -CH<sub>2</sub>Br), 7.46 (m, 1 H, C<sup>3</sup>H), 7.59 (m, 2 H, C<sup>5</sup>H, C<sup>4</sup>H), 7.87 (m, 1 H, C<sup>6</sup>H).

**Methyl-2-[(3-chlorophenoxy)methyl]benzoate (14).** K<sub>2</sub>CO<sub>3</sub> (2.42 g, 17.40 mmol) was suspended in acetone. Then 2.24 g (17.40 mmol) of 3-chlorophenol was added. After heating to 50 °C, 4.00 g (17.40 mmol) of methyl-2-(bromomethyl)-3-methoxybenzoate, dissolved in acetone, was added, and the mixture was heated for 6 h at 70 °C. After the reaction was completed, the solvent was removed, and the residue was dissolved in ethyl acetate. The organic layer was washed with 10% HCl and then dried over Na<sub>2</sub>SO<sub>4</sub>. The extract was further purified by flash chromatography (petrol ether/ethyl acetate, 3:1) to obtain a white oil. IR (ATR): 3403, 2961, 1711, 1432, 1265, 1034, 857, 761, 739, 677 cm<sup>-1</sup>. <sup>1</sup>H NMR (DMSO-*d*<sub>6</sub>) δ in ppm: 3.80 (s, 3 H, -OCH<sub>3</sub>), 5.42 (s, 2 H, CH<sub>2</sub>O), 6.99 (m, 3 H, C<sup>2</sup>H, C<sup>4</sup>H, C<sup>6</sup>H), 7.31 (m, 1 H, C<sup>3</sup>H), 7.47 (m, 1 H, C<sup>2</sup>H), 7.64 (m, 2 H, C<sup>4</sup>H, C<sup>3</sup>H), 7.90 (m, 1 H, C<sup>6</sup>H).

**[(3-Chlorophenoxy)methyl]benzoic acid (15).** Methyl-2-[(3-chlorophenoxy)methyl]benzoate (3.00 g, 10.87 mmol) was dissolved in 40 mL of methanol and heated to 50 °C until the solution was clear. Then 1.00 g (17.86 mmol) of KOH dissolved in 10 mL of H<sub>2</sub>O was added, and the reaction mixture was refluxed for 4 h. The solvent was then removed in vacuo, and the residue was dissolved in H<sub>2</sub>O. The solution was then acidified under ice cooling with 10% HCl, whereupon the product crystallized as a white solid. IR (ATR): 3343, 2970, 1587, 1565, 1272, 1231, 1113, 1039, 769, 738 cm<sup>-1</sup>. <sup>1</sup>H NMR (DMSO-*d*<sub>6</sub>) δ in ppm: 5.46 (s, 2 H, CH<sub>2</sub>O), 6.96 (d, *J* = 8.34 Hz, 1 H, C<sup>6</sup>H), 7.01 (d, *J* = 8.08 Hz, 1 H, C<sup>4</sup>H), 7.06 (s, 1 H, C<sup>2</sup>H), 7.33 (m, 1 H, C<sup>5</sup>H), 7.46 (m, 1 H, C<sup>3</sup>H), 7.61 (m, 2 H, C<sup>5</sup>H, C<sup>4</sup>H), 7.93 (d, *J* = 7.83 Hz, 1 H, C<sup>6</sup>H). <sup>13</sup>C NMR (DMSO-*d*<sub>6</sub>) δ in ppm: 68.0 (CH<sub>2</sub>O), 113.7 (C<sup>6</sup>), 114.8 (C<sup>2</sup>), 120.7 (C<sup>4</sup>), 127.8 (C<sup>5</sup>), 128.1 (C<sup>5</sup>), 129.7 (C<sup>1</sup>), 130.4 (C<sup>3</sup>), 130.9 (C<sup>4</sup>), 132.0 (C<sup>6</sup>), 133.7 (C<sup>2</sup>), 137.6 (C<sup>3</sup>), 159.3 (C<sup>1</sup>), 168.1 (CO<sub>2</sub>H).

**3-Chlorodibenzo[*b,e*]oxepin-11(6*H*)-one (16).** 2-(3-Chlorophenoxy)methylbenzoic acid (2.0 g, 7.36 mmol) was dissolved in 40 mL of dichloromethane and 1 mL of dimethylformamide and treated with 0.97 g (7.36 mmol) of oxalyl chloride. After 30 min of stirring, 2.30 g (17.30 mmol) of AlCl<sub>3</sub> was added to the mixture. After 30 min, the reaction mixture was hydrolyzed with H<sub>2</sub>O, and the organic layer was concentrated in vacuo. The extract was further purified by flash chromatography (petrol ether/ethyl acetate, 3:1) to obtain a white solid. IR (ATR): 3070, 1593, 1273, 1234, 1203, 1019, 874, 830, 756, 679 cm<sup>-1</sup>. <sup>1</sup>H NMR (DMSO-*d*<sub>6</sub>) δ in ppm: 5.34 (s, 2 H, C<sup>6</sup>H<sub>2</sub>), 7.22 (m, 2 H, C<sup>4</sup>H, C<sup>2</sup>H), 7.56 (m, 2 H, C<sup>9</sup>H, C<sup>7</sup>H), 7.67 (m, 1 H, C<sup>8</sup>H), 7.79 (d, *J* = 7.58 Hz, 1 H, C<sup>1</sup>H), 8.10 (d, *J* = 8.59 Hz, 1 H, C<sup>10</sup>H). <sup>13</sup>C NMR (DMSO-*d*<sub>6</sub>) δ in ppm: 73.0 (C<sup>6</sup>), 120.2 (C<sup>4</sup>), 122.5 (C<sup>2</sup>), 123.9 (C<sup>11a</sup>), 128.4, (C<sup>7</sup>) 128.9 (C<sup>9</sup>), 129.3 (C<sup>10</sup>), 133.1 (C<sup>8</sup>), 133.2 (C<sup>1</sup>), 135.6 (C<sup>10a</sup>), 139.6 (C<sup>6a</sup>), 139.7 (C<sup>3</sup>), 161.2 (C<sup>4a</sup>), 189.1 (C<sup>11</sup>).

***N*-[(3-(5-Oxo-10,11-dihydro-5*H*-dibenzo[*a,d*]cyclohepten-2-yl)amino)phenyl]benzamide (17).** Compound **17** was prepared according to general procedure A. The residue was purified by flash chromatography (*n*-hexane/ethyl acetate 1:1) to afford 145 mg (17%) as a yellow solid. Mp: 189 °C. IR (ATR): 3308, 1643, 1596, 1545, 1480, 1333, 1269, 1108, 861, 759, 691 cm<sup>-1</sup>. HPLC: 9.5 min (99.7%). <sup>1</sup>H NMR (DMSO-*d*<sub>6</sub>) δ in ppm: 3.08 (s, 4H), 6.93–7.06 (m, 3H), 7.28–7.59 (m, 8H), 7.80–8.03 (m, 5H), 8.90 (s, 1H, NH), 10.6 (s, 1H, NH). <sup>13</sup>C NMR (DMSO-*d*<sub>6</sub>) δ in ppm: 34.4, 36.1, 111.5, 113.4, 114.3, 114.9, 115.3, 126.8, 127.9, 128.0 (×2), 128.7 (×2), 129.1, 129.7, 130.4, 131.9, 132.2, 133.7, 135.4, 139.4, 140.4, 141.8, 142.0, 145.7, 148.5, 166.0, 191.2. HRMS-ESI, *m/z* (C<sub>28</sub>H<sub>22</sub>N<sub>2</sub>O<sub>2</sub>): calcd, 418.1681 [M + H]<sup>+</sup>; found, 418.1663.

***N*-[3-(5-Oxo-6,7,8,9-tetrahydro-5*H*-benzocyclohepten-2-ylamino)phenyl]benzamide (41).** Compound **41** was prepared according to general procedure B. The residue was purified by flash chromatography (*n*-hexane/ethyl acetate 3:2) to afford 118 mg (17.3%) as a yellow solid. Mp: 190 °C. IR (ATR): 3316, 2939, 2860, 1639, 1610, 1575, 1527, 1481, 1276, 861, 824, 690 cm<sup>-1</sup>. HPLC: 8.11

min (96.8%).  $^1\text{H}$  NMR (DMSO- $d_6$ )  $\delta$  in ppm: 1.77 (m, 4 H), 2.62 (t, 2 H,  $J_1 = 4.04$  Hz,  $J_2 = 6.44$  Hz), 8.56 (t, 2 H,  $J_1 = 5.92$  Hz,  $J_2 = 8.06$  Hz), 6.91–7.01 (m, 3 H), 7.22–7.39 (m, 2 H), 7.48–7.62 (m, 4 H), 7.78 (s, 1 H), 7.92–7.96 (m, 2 H), 8.73 (s, 1 H, NH), 10.22 (s, 1 H, NH).  $^{13}\text{C}$  NMR (DMSO- $d_6$ )  $\delta$  in ppm: 20.6, 25.0, 32.6, 41.1, 111.2, 113.0, 114.0, 114.9, 115.7, 128.0, 128.7, 129.1 (2 $\times$ ), 129.7 (2 $\times$ ), 130.9, 131.9, 135.4, 140.4, 142.1, 144.6, 148.1, 166.0, 202.2. HRMS-ESI,  $m/z$  ( $\text{C}_{24}\text{H}_{22}\text{N}_2\text{O}_2$ ): calcd, 370.1681 [M + H] $^+$ ; found, 370.1705.

**N-{3-[(11-Oxo-6,11-dihydrodibenzo[*b,e*]oxepin-3-yl)amino]phenyl}benzamide (73).** Compound 73 was prepared according to general procedure C. The residue was purified by flash chromatography (dichloromethane/ethanol 95:5) to afford 45 mg (13.2%) as a yellow solid. Mp: 97  $^\circ\text{C}$ . IR (ATR): 1588, 1562 1476, 1300, 1276, 1120, 871, 693  $\text{cm}^{-1}$ . HPLC: 7.92 min (100%).  $^1\text{H}$  NMR (DMSO- $d_6$ )  $\delta$  in ppm: 5.21 (s, 2 H,  $\text{C}^6\text{H}_2$ ), 6.65 (d,  $J = 2.02$  Hz, 1 H,  $\text{C}^4\text{H}$ ), 6.82 (d,  $J = 2.02$  Hz, 1 H,  $\text{C}^2\text{H}$ ), 6.92 (m, 1 H,  $\text{C}^2\text{H}$ ), 7.30 (m, 1 H,  $\text{C}^4\text{H}$ ), 7.51 (m, 7 H), 7.79 (m, 2 H,  $\text{C}^5\text{H}$ ,  $\text{C}^6\text{H}$ ,  $\text{C}^7\text{H}$ ,  $\text{C}^9\text{H}$ ,  $\text{C}^{10}\text{H}$ ,  $\text{C}^8\text{H}$ ,  $\text{C}^4\text{H}$ ), 7.83 (m, 2 H,  $\text{C}^3\text{H}$ ,  $\text{C}^5\text{H}$ ), 7.94 (m, 2 H,  $\text{C}^2\text{H}$ ,  $\text{C}^6\text{H}$ ), 8.03 (d,  $J = 8.97$  Hz, 1 H,  $\text{C}^{10}\text{H}$ ), 9.05 (s, NH, 1 H) 10.27 (s, NH, 1 H).  $^{13}\text{C}$  NMR (DMSO- $d_6$ )  $\delta$  in ppm: 73.1 ( $\text{C}^6$ ), 102.7 ( $\text{C}^4$ ), 110.9 ( $\text{C}^2$ ), 111.9 ( $\text{C}^6$ ), 114.8 ( $\text{C}^2$ ), 115.8 ( $\text{C}^4$ ), 117.1 ( $\text{C}^{11a}$ ), 128.0 ( $\text{C}^2$ ,  $\text{C}^5$ ), 128.4 ( $\text{C}^7$ ), 128.7 ( $\text{C}^3$ ,  $\text{C}^6$ ), 129.2 ( $\text{C}^9$ ), 129.3 ( $\text{C}^5$ ), 129.8 ( $\text{C}^{10}$ ), 131.9 ( $\text{C}^8$ ), 132.6 ( $\text{C}^1$ ), 133.7 ( $\text{C}^{10a}$ ), 135.3 ( $\text{C}^{10a}$ ), 136.3 ( $\text{C}^1$ ), 140.5 ( $\text{C}^3$ ), 141.3 ( $\text{C}^{6a}$ ), 151.2 ( $\text{C}^3$ ), 163.2 ( $\text{C}^{4a}$ ), 166.0 ( $\text{C}=\text{O}_{\text{amide}}$ ), 187.5 ( $\text{C}^{11}$ ). HRMS-ESI,  $m/z$  ( $\text{C}_{27}\text{H}_{20}\text{N}_2\text{O}_3$ ): calcd, 443.1366 [M + Na] $^+$ ; found, 443.1364.

**Crystallization and Structure Determination of p38 $\alpha$  MAP Kinase in Complex with Compound 45.** Inactive (nonphosphorylated) human p38 $\alpha$  MAP kinase was expressed and purified as described previously.<sup>42</sup> The purified protein was concentrated to 14 mg/mL and flash frozen in liquid nitrogen. Protein crystals of p38 $\alpha$  MAP kinase were obtained using crystallization conditions similar to those previously reported.<sup>43</sup> Briefly, apo-crystals of p38 $\alpha$  were grown in 24-well crystallization plates using the hanging-drop vapor diffusion method at 20  $^\circ\text{C}$  by mixing 1  $\mu\text{L}$  of protein solution (14 mg/mL) with 1  $\mu\text{L}$  of reservoir solution (100 mM MES, pH 6.0–6.3, 22–27% PEG4000, 50 mM *n*-octyl- $\beta$ -D-glucopyranoside). For soaking experiments, 20  $\mu\text{L}$  of reservoir solution was mixed with 0.2  $\mu\text{L}$  of compound 45 (100 mM in DMSO) and centrifuged for 5 min at 13 000 rpm to remove excess compound. Apo-crystals were transferred to a new drop (1  $\mu\text{L}$ ) of this solution and incubated at 20  $^\circ\text{C}$  for 24 h. Crystals were cryoprotected by addition of 25% PEG400 and subsequently flash frozen in liquid nitrogen.

Diffraction data were collected at the PX10SA beamline of the Swiss Light Source (PSI, Villigen, Switzerland) to a resolution of 2.4  $\text{Å}$  using wavelengths close to 1  $\text{Å}$ . Images were processed with XDS and scaled using XSCALE.<sup>44</sup>

**Structure Determination and Refinement of p38 $\alpha$  with Compound 45.** The p38 $\alpha$ –inhibitor complex structure was obtained by molecular replacement with PHASER,<sup>45</sup> using a related p38 $\alpha$  MAP kinase structure (Protein Data Bank entry 3QUE<sup>24</sup>) as a search model. Crystallographic refinement was performed with CNS<sup>46</sup> and Refmac5.<sup>47</sup> Model building and real space refinement was done using the program COOT.<sup>48</sup> The topology and library files for the ligand were generated with the Dundee PRODRG server.<sup>49</sup> The refined structure was validated with PROCHECK.<sup>50</sup> Detailed data, refinement, and geometry statistics are provided in Table 4. The graphics were obtained using PyMOL 1.5.0.4.

## ■ ASSOCIATED CONTENT

### 📄 Supporting Information

Experimental and analytical data, including HPLC purity and HRMS data of compounds 17–88 and selectivity profile of compound 45. This material is available free of charge via the Internet at <http://pubs.acs.org>.

### Accession Codes

A new structure of the human p38 $\alpha$  MAP kinase in complex with compound 45 is deposited under the accession code 3UVP in the Protein Data Bank.

## ■ AUTHOR INFORMATION

### Corresponding Author

\*E-mail: stefan.laufer@uni-tuebingen.de. Telephone: +49-7071-2972459. Telefax: +49-7071-295037.

### Notes

The authors declare no competing financial interest.

## ■ ACKNOWLEDGMENTS

The authors want to thank Katharina Bauer for biological testing and Ida D’Orazio for the synthesis of compounds 57 and 80.

## ■ REFERENCES

- Dalrymple, S. A. p38 mitogen activated protein kinase as a therapeutic target for Alzheimer’s disease. *J. Mol. Neurosci.* **2002**, *19*, 295–299.
- den Broeder, A.; van de Putte, L.; Rau, R.; Schattenkirchner, M.; Van Riel, P.; Sander, O.; Binder, C.; Fenner, H.; Bankmann, Y.; Velagapudi, R.; Kempeni, J.; Kupper, H. A single dose, placebo controlled study of the fully human anti-tumor necrosis factor-alpha antibody adalimumab (D2E7) in patients with rheumatoid arthritis. *J. Rheumatol.* **2002**, *29*, 2288–2298.
- Feldmann, M.; Brennan, F. M.; Maini, R. N. Rheumatoid arthritis. *Cell* **1996**, *85*, 307–310.
- Mikuls, T. R.; Moreland, L. W. TNF blockade in the treatment of rheumatoid arthritis: infliximab versus etanercept. *Expert Opin. Pharmacother.* **2001**, *2*, 75–84.
- Cohen, S.; Hurd, E.; Cush, J.; Schiff, M.; Weinblatt, M. E.; Moreland, L. W.; Kremer, J.; Bear, M. B.; Rich, W. J.; McCabe, D. Treatment of rheumatoid arthritis with anakinra, a recombinant human interleukin-1 receptor antagonist, in combination with methotrexate: Results of a twenty-four-week, multicenter, randomized, double-blind, placebo-controlled trial. *Arthritis Rheum.* **2002**, *46*, 614–624.
- Lee, J. C.; Laydon, J. T.; McDonnell, P. C.; Gallagher, T. F.; Kumar, S.; Green, D.; McNulty, D.; Blumenthal, M. J.; Heys, J. R.; Landvatter, S. W. A protein kinase involved in the regulation of inflammatory cytokine biosynthesis. *Nature* **1994**, *372*, 739–746.
- Karcher, S. C.; Laufer, S. A. Successful structure-based design of recent p38 MAP kinase inhibitors. *Curr. Top. Med. Chem. (Sharjah, United Arab Emirates)* **2009**, *9*, 655–676.
- Lee, M. R.; Dominguez, C. MAP kinase p38 inhibitors: Clinical results and an intimate look at their interactions with p38alpha protein. *Curr. Med. Chem.* **2005**, *12*, 2979–2994.
- Liu, Y.; Gray, N. S. Rational design of inhibitors that bind to inactive kinase conformations. *Nat. Chem. Biol.* **2006**, *2*, 358–364.
- Pettus, L. H.; Wurz, R. P. Small molecule p38 MAP kinase inhibitors for the treatment of inflammatory diseases: novel structures and developments during 2006–2008. *Curr. Top. Med. Chem.* **2008**, *8*, 1452–1467.
- Kumar, S.; Jiang, M. S.; Adams, J. L.; Lee, J. C. Pyridinylimidazole compound SB 203580 inhibits the activity but not the activation of p38 mitogen-activated protein kinase. *Biochem. Biophys. Res. Commun.* **1999**, *263*, 825–831.
- Kumar, S.; Boehm, J.; Lee, J. C. p38 MAP kinases: Key signalling molecules as therapeutic targets for inflammatory diseases. *Nat. Rev. Drug Discovery* **2003**, *2*, 717–726.
- Moran, N. p38 kinase inhibitor approved for idiopathic pulmonary fibrosis. *Nat. Biotechnol.* **2011**, *29*, 301.
- Xing, L.; Shieh, H. S.; Selness, S. R.; Devraj, R. V.; Walker, J. K.; Devadas, B.; Hope, H. R.; Compton, R. P.; Schindler, J. F.; Hirsch, J. L.; Benson, A. G.; Kurumbail, R. G.; Stegeman, R. A.; Williams, J. M.; Broadus, R. M.; Walden, Z.; Monahan, J. B. Structural bioinformatics-based prediction of exceptional selectivity of p38 MAP kinase inhibitor PH-797804. *Biochemistry* **2009**, *48*, 6402–6411.
- Pharmacia & Upjohn Co.LLC. Crystalline forms of 3-[5-chloro-4-[(2,4-difluorobenzyl)oxy]-6-oxopyrimidin-1(6H)-YL]-N-(2-hydrox-

- yethyl)-4-methylbenzamide. International Patent WO2006040649, 2006.
- (16) Pharmacia Corp. Diaryl substituted pyridinones. U.S. Patent US2006211694, 2006.
- (17) Pharmacia Corp. Substituted pyrimidinones. U.S. Patent US7795271, 2010.
- (18) Norman, P. BMS-582949: crystalline form of a p38alpha inhibitor? WO2008079857. *Expert Opin. Ther. Pat.* **2009**, *19*, 1165–1168.
- (19) Malley, M. F. (Bristol-Myers Squibb Company, USA) Crystalline forms of an aryl-substituted pyrazoleamide. International Patent WO 2008079857. 2008.
- (20) Liu, C.; Lin, J.; Wroblewski, S. T.; Lin, S.; Hynes, J.; Wu, H.; Dyckman, A. J.; Li, T.; Wityak, J.; Gillooly, K. M.; Pitt, S.; Shen, D. R.; Zhang, R. F.; McIntyre, K. W.; Salter-Cid, L.; Shuster, D. J.; Zhang, H.; Marathe, P. H.; Doweiko, A. M.; Sack, J. S.; Kiefer, S. E.; Kish, K. F.; Newitt, J. A.; McKinnon, M.; Dodd, J. H.; Barrish, J. C.; Schieven, G. L.; Leftheris, K. Discovery of 4-(5-(cyclopropylcarbamoyl)-2-methylphenylamino)-5-methyl-N-propylpyrrolo[1,2-f][1,2,4]triazine-6-carboxamide (BMS-582949), a clinical p38 $\alpha$  MAP kinase inhibitor for the treatment of inflammatory diseases. *J. Med. Chem.* **2010**, *53*, 6629–6639.
- (21) Lee, J. C.; Kassis, S.; Kumar, S.; Badger, A.; Adams, J. L. p38 mitogen-activated protein kinase inhibitors—mechanisms and therapeutic potentials. *Pharmacol. Ther.* **1999**, *82*, 389–397.
- (22) Fischer, S.; Koeberle, S. C.; Laufer, S. A. p38alpha mitogen-activated protein kinase inhibitors, a patent review. *Expert Opin. Ther. Pat.* **2011**, *21*, 1843–1866.
- (23) Laufer, S. A.; Ahrens, G. M.; Karcher, S. C.; Hering, J. S.; Niess, R. Design, synthesis, and biological evaluation of phenylamino-substituted 6,11-dihydro-dibenzo[*b,e*]oxepin-11-ones and dibenzo[*a,d*]cycloheptan-5-ones: Novel p38 MAP kinase inhibitors. *J. Med. Chem.* **2006**, *49*, 7912–7915.
- (24) Koeberle, S. C.; Romir, J.; Fischer, S.; Koeberle, A.; Schattel, V.; Albrecht, W.; Grutter, C.; Werz, O.; Rauh, D.; Stehle, T.; Laufer, S. A. Skepinone-L is a selective p38 mitogen-activated protein kinase inhibitor. *Nat. Chem. Biol.* **2011**, *8*, 141–143.
- (25) Murineddu, G.; Ruiu, S.; Loriga, G.; Manca, I.; Lazzari, P.; Reali, R.; Pani, L.; Toma, L.; Pinna, G. A. Tricyclic pyrazoles. 3. Synthesis, biological evaluation, and molecular modeling of analogues of the cannabinoid antagonist 8-chloro-1-(2',4'-dichlorophenyl)-N-piperidin-1-yl-1,4,5,6-tetrahydrobenzo[6,7]cyclohepta[1,2-c]pyrazole-3-carboxamide. *J. Med. Chem.* **2005**, *48*, 7351–7362.
- (26) Engelhardt, E. L.; Zell, H. C.; Saari, W. S.; Christy, M. E.; Colton, C. D.; Stone, C. A.; Stavorski, J. M.; Wenger, H. C.; Ludden, C. T. Structure–activity relationships in the cyproheptadine series. *J. Med. Chem.* **1965**, *8*, 829–835.
- (27) Kurokawa, M.; Sato, F.; Masuda, Y.; Yoshida, T.; Ochi, Y.; Zushi, K.; Fujiwara, I.; Naruto, S.; Uno, H.; Matsumoto, J. Synthesis and biological activity of 11-[4-(cinnamyl)-1-piperazinyl]-6,11-dihydrodibenz[*b,e*]oxepin derivatives, potential agents for the treatment of cerebrovascular disorders. *Chem. Pharm. Bull. (Tokyo)* **1991**, *39*, 2564–2573.
- (28) Schrödinger Suite 2008 Induced Fit Docking protocol. [Glide version 5.0] Schrödinger, LLC, New York, NY, 2005.
- (29) Jensen, T. A.; Liang, X.; Tanner, D.; Skjaerbaek, N. Rapid and efficient microwave-assisted synthesis of aryl aminobenzophenones using Pd-catalyzed amination. *J. Org. Chem.* **2004**, *69*, 4936–4947.
- (30) Goettert, M.; Graeser, R.; Laufer, S. A. Optimization of a nonradioactive immunosorbent assay for p38alpha mitogen-activated protein kinase activity. *Anal. Biochem.* **2010**, *406*, 233–234.
- (31) Angell, R.; Aston, N. M.; Bamborough, P.; Buckton, J. B.; Cockerill, S.; deBoeck, S. J.; Edwards, C. D.; Holmes, D. S.; Jones, K. L.; Laine, D. I.; Patel, S.; Smea, P. A.; Smith, K. J.; Somers, D. O.; Walker, A. L. Biphenyl amide p38 kinase inhibitors 3: Improvement of cellular and in vivo activity. *Bioorg. Med. Chem. Lett.* **2008**, *18*, 4428–4432.
- (32) Backes, A. C.; Zech, B.; Felber, B.; Klebl, B.; Mueller, G. Small-molecule inhibitors binding to protein kinases. Part I: exceptions from the traditional pharmacophore approach of type I inhibition. *Expert Opin. Drug Discovery* **2012**, *3*, 1409–1425.
- (33) Backes, A. C.; Zech, B.; Felber, B.; Klebl, B.; Mueller, G. Small-molecule inhibitors binding to protein kinase. Part II: the novel pharmacophore approach of type II and type III inhibition. *Expert Opin. Drug Discovery* **2008**, *3*, 1427–1449.
- (34) Cogan, D. A.; Aungst, R.; Breinlinger, E. C.; Fadra, T.; Goldberg, D. R.; Hao, M. H.; Kroe, R.; Moss, N.; Pargellis, C.; Qian, K. C.; Swinamer, A. D. Structure-based design and subsequent optimization of 2-tolyl-(1,2,3-triazol-1-yl)-4-carboxamide inhibitors of p38 MAP kinase. *Bioorg. Med. Chem. Lett.* **2008**, *18*, 3251–3255.
- (35) Wroblewski, S. T.; Lin, S.; Hynes, J., Jr.; Wu, H.; Pitt, S.; Shen, D. R.; Zhang, R.; Gillooly, K. M.; Shuster, D. J.; McIntyre, K. W.; Doweiko, A. M.; Kish, K. F.; Tredup, J. A.; Duke, G. J.; Sack, J. S.; McKinnon, M.; Dodd, J.; Barrish, J. C.; Schieven, G. L.; Leftheris, K. Synthesis and SAR of new pyrrolo[2,1-f][1,2,4]triazines as potent p38 alpha MAP kinase inhibitors. *Bioorg. Med. Chem. Lett.* **2008**, *18*, 2739–2744.
- (36) www.proqinase.com. 2012.
- (37) Scios Inc. Indole-type inhibitors of p38 kinase. U.S. Patent US6890938. 2005.
- (38) Simard, J. R.; Getlik, M.; Grutter, C.; Schneider, R.; Wulfert, S.; Rauh, D. Fluorophore labeling of the glycine-rich loop as a method of identifying inhibitors that bind to active and inactive kinase conformations. *J. Am. Chem. Soc.* **2010**, *132*, 4152–4160.
- (39) Boehringer Ingelheim Pharma. Methods of treating COPD and pulmonary hypertension. International Patent WO200501862. 2005.
- (40) Ahn, Y. M.; Clare, M.; Ensinger, C. L.; Hood, M. M.; Lord, J. W.; Lu, W. P.; Miller, D. F.; Patt, W. C.; Smith, B. D.; Vogeti, L.; Kaufman, M. D.; Petillo, P. A.; Wise, S. C.; Abendroth, J.; Chun, L.; Clark, R.; Feese, M.; Kim, H.; Stewart, L.; Flynn, D. L. Switch control pocket inhibitors of p38-MAP kinase. Durable type II inhibitors that do not require binding into the canonical ATP hinge region. *Bioorg. Med. Chem. Lett.* **2010**, *20*, 5793–5798.
- (41) Getlik, M.; Grutter, C.; Simard, J. R.; Nguyen, H. D.; Robubi, A.; Aust, B.; van Otterlo, W. A.; Rauh, D. Structure-based design, synthesis and biological evaluation of N-pyrazole, N'-thiazole urea inhibitors of MAP kinase p38alpha. *Eur. J. Med. Chem.* **2012**, *48*, 1–15.
- (42) Simard, J. R.; Getlik, M.; Grutter, C.; Pawar, V.; Wulfert, S.; Rabiller, M.; Rauh, D. Development of a fluorescent-tagged kinase assay system for the detection and characterization of allosteric kinase inhibitors. *J. Am. Chem. Soc.* **2009**, *131*, 13286–13296.
- (43) Bukhtiyarova, M.; Northrop, K.; Chai, X.; Casper, D.; Karpusas, M.; Springman, E. Improved expression, purification, and crystallization of p38alpha MAP kinase. *Protein Expression Purif.* **2004**, *37*, 154–161.
- (44) Kabsch, W. Automatic processing of rotation diffraction data from crystals of initially unknown symmetry and cell constants. *J. Appl. Crystallogr.* **1993**, *26*, 795–800.
- (45) Read, R. J. Pushing the boundaries of molecular replacement with maximum likelihood. *Acta Crystallogr., Sect. D: Biol. Crystallogr.* **2001**, *57*, 1373–1382.
- (46) Brunger, A. T.; Adams, P. D.; Clore, G. M.; DeLano, W. L.; Gros, P.; Grosse-Kunstleve, R. W.; Jiang, J. S.; Kuszewski, J.; Nilges, M.; Pannu, N. S.; Read, R. J.; Rice, L. M.; Simonson, T.; Warren, G. L. Crystallography & NMR system: A new software suite for macromolecular structure determination. *Acta Crystallogr., Sect. D: Biol. Crystallogr.* **1998**, *54*, 905–921.
- (47) Murshudov, G. N.; Vagin, A. A.; Dodson, E. J. Refinement of macromolecular structures by the maximum-likelihood method. *Acta Crystallogr., Sect. D: Biol. Crystallogr.* **1997**, *53*, 240–255.
- (48) Emsley, P.; Cowtan, K. Coot: Model-building tools for molecular graphics. *Acta Crystallogr., Sect. D: Biol. Crystallogr.* **2004**, *60*, 2126–2132.
- (49) Schuttelkopf, A. W.; van Aalten, D. M. PRODRG: A tool for high-throughput crystallography of protein-ligand complexes. *Acta Crystallogr., Sect. D: Biol. Crystallogr.* **2004**, *60*, 1355–1363.

(50) Laskowski, R. A.; MacArthur, M. W.; Moss, D. S.; Thornton, J. M. PROCHECK: A program to check the stereochemical quality of protein structures. *J. Appl. Crystallogr.* **1993**, *26*, 283–291.